Coupling of small, low-loss hexapole mode with photonic crystal slab waveguide mode

Guk-Hyun Kim and Yong-Hee Lee

Department of Physics, Korea Advanced Institute of Science and Technology, Daejeon 305-701, Korea
tan@kaist.ac.kr

Akihiko Shinya and Masaya Notomi

NTT Basic Research Laboratories, NTT Corporation, 3-1 Morinosato-Wakamiya, Atsugi 243-0198, Japan

Abstract: Coupling characteristics between the single-cell hexapole mode and the triangular-lattice photonic crystal slab waveguide mode is studied by the finite-difference time-domain method. The single-cell hexapole mode has a high quality factor (Q) of 3.3×10^6 and a small modal volume of $1.18(\lambda/n)^3$. Based on the symmetry, three representative types of coupling geometries (shoulder-couple, butt-couple and side-couple structures) are selected and tested. The coupling efficiency shows strong dependence on the transverse overlap of the cavity mode and the waveguide mode over the region of the waveguide. The shoulder-couple structure shows best coupling characteristics among three tested structures. For example, two shoulder-couple waveguides and a hexapole cavity result in a high performance resonant-tunneling-filter with Q of 9.7×10^5 and transmittance of 0.48. In the side-couple structure, the coupling strength is much weaker than that of the shoulder-couple structure because of the poor spatial overlap between the mode profiles. In the direct-couple structure, the energy transfer from the cavity to the waveguide is prohibited because of the symmetry mismatch and no coupling is observed.

OCIS codes: (250.5300) Photonic integrated circuits; (230.5750) Resonators; (230.7370) Waveguides

References and links

1. H. Y. Ryu, S. H. Kim, H. G. Park, J. K. Hwang, Y. H. Lee, and J. S. Kim, "Square-lattice photonic band-gap single-cell laser operating in the lowest-order whispering gallery mode," Appl. Phys. Lett. **80**, 3883-3885 (2002).
2. K. Srinivasan and O. Painter, "Momentum space design of high-Q photonic crystal optical cavities," Opt. Express **10**, 670-684 (2002), http://www.opticsexpress.org/abstract.cfm?URI=OPEX-10-15-670.
3. J. Vučković and Y. Yamamoto, "Photonic crystal microcavities for cavity quantum electrodynamics with a single quantum dot," Appl. Phys. Lett. **82**, 2374-2376 (2003).
4. Y. Akahane, T. Asano, B. S. Song, and S. Noda, "High-Q photonic nanocavity in a two-dimensional photonic crystal," Nature **425**, 944-947 (2003).
5. H. Y. Ryu, M. Notomi, and Y. H. Lee, "High-quality-factor and small-mode-volume hexapole modes in photonic-crystal-slab nanocavities," Appl. Phys. Lett. **83**, 4294-4296 (2003).
6. S. Noda, A. Chutinan, and M. Imada, "Trapping and emission of photons by a single defect in a photonic bandgap structure," Nature **407**, 608-610 (2000).
7. H. Takano, Y. Akahane, T. Asano, and S. Noda, "In-plane-type channel drop filter in a two-dimensional photonic crystal slab," Appl. Phys. Lett. **84**, 2226-2228 (2004).
8. M. Notomi, A. Shinya, S. Mitsugi, E. Kuramochi, and H. Y. Ryu, "Waveguides, resonators and their coupled elements in photonic crystal slabs," Opt. Express **12**, 1551-1561 (2004) http://www.opticsexpress.org/abstract.cfm?URI=OPEX-12-8-1551.
9. M. F. Yanki, S. Fan, M. Soljačić, and J. D. Joannopoulos, "All-optical transistor action with bistable switching in a photonic crystal cross-waveguide geometry," Opt. Lett. **28**, 2506-2508 (2003).

#5765 - $15.00 US Received 17 November 2004; revised 13 December 2004; accepted 16 December 2004

10. M. F. Yanki, S. Fan, and M. Soljačić, "High-contrast all-optical bistable switching in photonic crystal microcavities," Appl. Phys. Lett. **83**, 2739-2741 (2003).
11. C. J. M. Smith, R. M. De La Rue, M. Rattier, S. Olivier, H. Benisty, C. Weisbuch, T. F. Krauss, R. Houdré, and U. Oesterle, "Coupled guide and cavity in a two-dimensional photonic crystal," Appl. Phys. Lett. **78**, 1487-1489 (2001).
12. C. Seassal, Y. Désières, X. Letartre, C. Grillet, P. Rojo-Romeo, P. Viktorovitch, and T. Benyattou, "Optical coupling between a two-dimensional photonic crystal-based microcavity and single-line defect waveguide on InP membranes," IEEE J. Quantum Electron. **38**, 811-815 (2002).
13. P. E. Barclay, K. Srinivasan, and O. Painter, "Design of photonic crystal waveguides for evanescent coupling to optical fiber tapers and integration with high-*Q* cavities," J. Opt. Soc. Am. B **20**, 2274-2284 (2003).
14. M. Notomi, K. Yamada, A. Shinya, J. Takahashi, C. Takahashi, and I. Yokohama, "Extremely large group velocity dispersion of line-defect waveguides in photonic crystal slabs," Phys. Rev. Lett. **87**, 253902 (2001).
15. C. Manolatou, M. J. Khan, S. Fan, P. R. Villeneuve, H. A. Haus, and J. D. Joannopoulos, "Coupling of modes analysis of resonant channel add-drop filters," IEEE J. Quantum Electron. **35**, 1322-1331 (1999).

1. Introduction

The two-dimensional slab photonic crystal (PhC) cavity is known to be advantageous to construct a high quality factor (Q) resonant mode with a small modal volume (V) [1-5]. If efficient ways to funnel the energy of the resonator into PhC waveguides are found, the large-Q/V resonator can be used for applications such as high-performance filters[6-8] and ultra-small all-optical switches [9,10]. Therefore, understanding of the basic mechanisms of the cavity-waveguide coupling becomes an important issue for PhC-based optical circuits [8,11-13].

In the previous work [5], the hexapole mode was reported to have a high Q of ~10^6 with a small V of ~$1.0(\lambda/n)^3$. (The λ is the resonant wavelength and the n is the refractive index of the slab material.) The very large Q/V value drew attentions of research communities. Here, we design a modified-single-cell, high-Q, small-V hexapole mode cavity and a PhC waveguide to study energy exchanges between the cavity and the waveguide. The hexapole mode has six arms along Γ-M directions of triangular lattice as shown Fig. 2(b). The six-fold symmetry limits the number of possible coupling configurations. Based on the symmetry argument, three representative coupling geometries are selected and investigated by the finite-difference time-domain method.

2. High-*Q*, small-volume hexapole mode

The modified single-cell cavity tested is shown in Fig. 1(a). In the structure, the six nearest-neighbor holes (NNHs) are made small and pushed away from the center of symmetry. As the size of the modified single-cell cavity increases, the hexapole mode is pulled down from the air-band [5]. Note that the cavity still has the hexagonal symmetry. Structural variable parameters of the cavity are the radius (r_n) of NNH and the distance (c_n) between the cavity center and the NNH center. The thickness of slab and the radius of air hole constituting the triangular-lattice PhC slab are fixed to 0.5a and 0.25a, respectively. (The a is the lattice constant.) The refractive index of the slab material is 3.46, which corresponds to silicon at λ=1.55μm. When c_n=1.18a and r_n=0.21~0.25a, the vertical quality factor (Q_V) and the modal volume (V) are plotted in Fig. 1(b). Here, we assume an infinite horizontal quality factor (Q_H) because the size of surrounding PhC is sufficiently large (~50a×50a). Under this condition, Q_V becomes the total quality factor (Q_T). The highest Q_V of 3.3×10^6 with a V of $1.18(\lambda/n)^3$ is achieved when r_n=0.23a. These values are comparable to those of the previous work [5]. This hexapole mode is to be coupled with PhC waveguide modes.

#5765 - $15.00 US Received 17 November 2004; revised 13 December 2004; accepted 16 December 2004

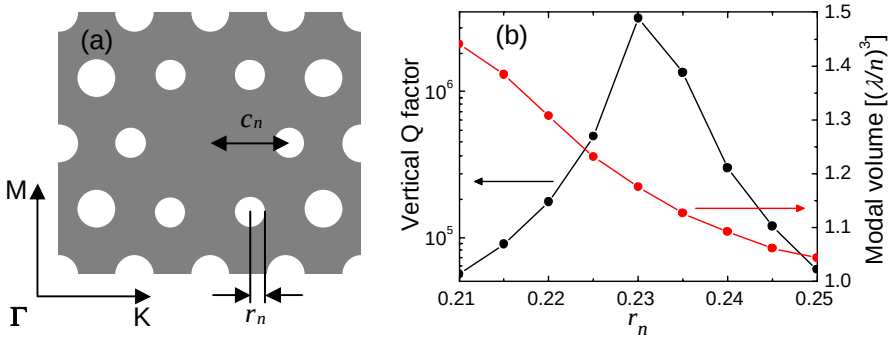

Fig. 1. (a) Modified single-cell cavity structure. Six nearest-neighbor holes (NNHs) are reduced and pushed away from the cavity center. r_n and c_n denote the radius of NNH and the distance between the cavity center and NNH center, respectively. (b) Vertical quality factor (Q_V) and modal volume (V) of isolated hexapole mode when c_n=1.18a and r_n=0.21~0.25a. Black and red lines represent Q_V and V, respectively.

The H_Z (z-component of magnetic field) distribution of the hexapole mode is shown in Fig. 2(a). In general, the weak outer portion of the hexapole mode that overlaps with the nearby photonic crystal waveguide, is responsible for the cavity-waveguide coupling. In order to describe the weak amplitude of the mode faithfully, the saturated dual color coding scheme is employed as shown in Fig. 2(b). The red and blue colors represent positive and negative amplitudes. Each color is mixed linearly with a white color to represent those regions that have amplitudes smaller than 1/20 of the maximum value. All the other parts that have amplitudes larger than 1/20 of the maximum value have saturated blue or red color.

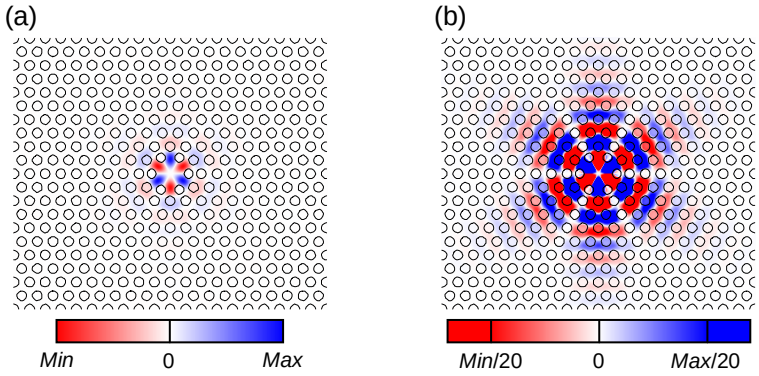

Fig. 2. (a) H_Z (z-component of magnetic field) distribution of hexapole mode when c_n=1.18a and r_n=0.23a. (b) Red or blue color is mixed linearly with a white color to represent those regions that have amplitudes smaller than 1/20 of the maximum value. All the other parts that have amplitudes larger than 1/20 of the maximum value have saturated blue or red color.

3. PhC waveguide mode

The basic waveguide is a Γ-K directional waveguide formed by filling in one row of air holes. Dispersion characteristics of the PhC waveguide are plotted in Fig. 3(a) [14]. To avoid the modal dispersion in waveguide structure, an optical signal should propagate in a single-mode waveguide. And to send a photon over a long distance, the waveguide mode should have low propagation losses. Those waveguide modes in the frequency range of 0.262~0.275a/λ satisfy the above requirements. However, the hexapole mode is out of this frequency range. Therefore, we shift up the dispersion curve of the waveguide by modifying the first side-hole at both sides as in Fig. 3(b). Remember that the conditions of the hexapole mode have already been optimized for the best quality factor and the resonant frequency has been fixed. Fig. 3(c)

#5765 - $15.00 US Received 17 November 2004; revised 13 December 2004; accepted 16 December 2004

shows the dispersion of the PhC waveguide when the radius (r_w) of the first side-hole at both sides is slightly increased to 0.30a from the original value of 0.25a. Now the cross-point of the hexapole mode and waveguide modes is just one and it is below the light line. Note that as shown in Fig. 3(d), the H_Z distribution of the PhC waveguide mode at the cross-point has the even symmetry with respect to the waveguide axis and the wave vector is 0.31a/λ. Figure 3(a) and Fig. 3(c) show that only even waveguide-mode is the candidate to satisfy the two requirements mentioned above. Forget the odd waveguide-mode and focus only on the even waveguide-mode.

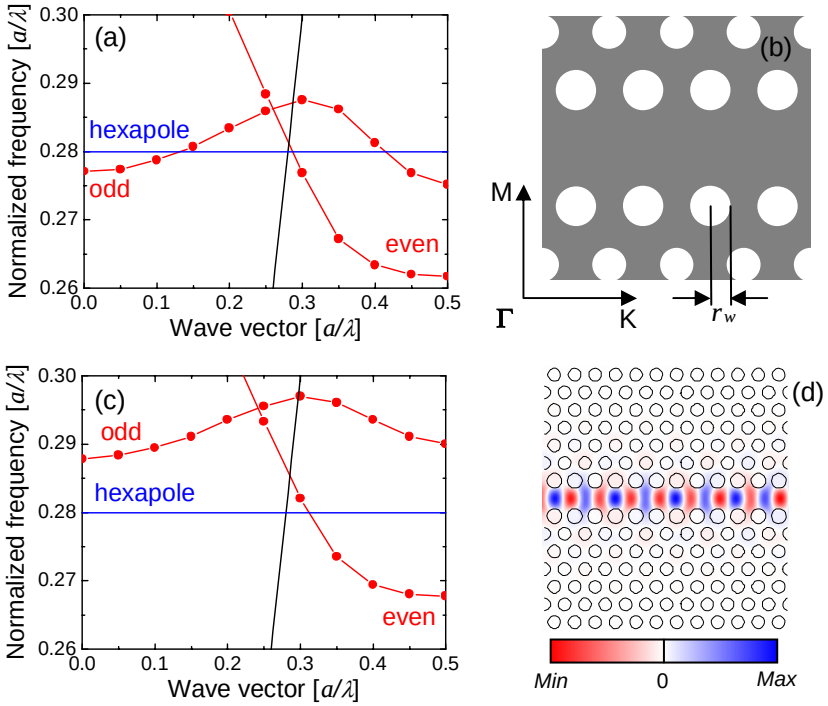

Fig. 3. (a) Dispersion curve of Γ-K directional PhC waveguide formed by filling in one row of air holes. Blue line represents the hexapole mode frequency. Black line is the light line. (b) Modified Γ-K directional PhC waveguide structure. The first side-hole is enlarged at both sides. r_w denotes the radius of the first side-hole. (c) Dispersion curve of modified Γ-K directional PhC waveguide with r_w=0.3a. (d) H_Z distribution of waveguide mode at cross-point of blue and red lines in (c).

4. Cavity-waveguide coupled structures

Various cavity-waveguide coupled geometries based on the modified single-cell cavity (c_n=1.18a and r_n=0.23a) and the modified PhC waveguide (r_w=0.30a) are investigated. Coupling characteristics between modes depend on both the spectral match and the spatial overlap of the two field distributions. Compare the field distributions of the hexapole mode and even waveguide-mode of Fig. 2(b) and Fig. 3(d). Considering the field distribution and symmetry, three representative cavity-waveguide coupled structures are selected as shown in Fig. 4(a), Fig. 5(a) and Fig. 6(a). The position of the coupling waveguide with respect to the arm of the hexapole mode is different in each case. They are named as shoulder-couple, butt-couple and side-couple structures, respectively. When a waveguide is introduced near a resonant mode, it can induce the energy-flow into the waveguide and the in-plane scattering loss through the surrounding PhC. We have calculated the energy-flow and the in-plane scattering loss. According to our calculations, the in-plane loss is negligible and the energy-flow into waveguide can be represented by the horizontal quality factor (Q_H).

#5765 - $15.00 US Received 17 November 2004; revised 13 December 2004; accepted 16 December 2004

5. Shoulder-couple structure

The H_Z distribution of the hexapole mode excited in the shoulder-couple structure is shown in Fig. 4(a). In this configuration, the resonant cavity is placed between two terminated Γ-K waveguides that are displaced along the Γ-M direction. The whole structure is symmetric with respect to its center. Some energy of the hexapole mode is expected to flow horizontally into the nearby waveguides and the mode would have the different characteristics from those of the isolated mode.

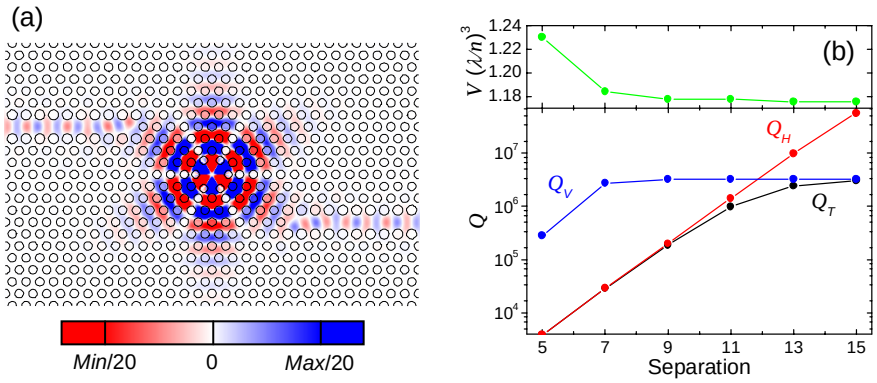

Fig. 4. (a) Shoulder-couple structure of separation=7 with H_Z distribution. (b) Modal volume (V) and quality factors (Qs) of hexapole mode. Green line represents modal volume. Black, red and blue lines represent total, horizontal and vertical Qs, respectively.

We investigate coupling characteristics of shoulder-couple structure as a function of separation. The separation is represented as the number of air-hole rows between the center of the cavity and the end of the PhC waveguide. For example, the separation is 7 in Fig. 4(a). The modal volume and three differentiable quality factors are plotted in Fig. 4(b). The Q_T, Q_H and Q_V correspond to the decay of hexapole-mode energy into the whole space, two waveguides and air, respectively. Especially, the coupling between the hexapole mode and the even waveguide-mode can be represented by the horizontal quality factor Q_H. As the separation increases, the in-plane waveguide coupling decreases exponentially. And the Q_V approaches the value of the isolated hexapole mode when the separation is ≥7, while keeping the modal volume almost identical to that of the isolated hexapole mode. In this shoulder-couple structure, the hexapole mode smoothly couples with the waveguide mode maintaining its advantages of high Q_V and small V. We have also examined other possible configurations of the shoulder-couple scheme in which the angle between axes of two waveguides is 60° or 120°. They had the almost same characteristics as the basic configuration of Fig. 4(a).

The transverse overlap of the cavity mode and the waveguide mode over the region of the waveguide is a key factor that determines the coupling characteristics [13]. If the transverse-directional overlap is poor, the efficient coupling is not achieved. Actually, such situation appears in next cases of the butt-couple and the side-couple. In the shoulder-coupling structure, the decaying direction of the hexapole-mode arm has a tilt to the waveguide axis as shown in Fig. 4(a). The tilted join removes the possibility of the poor overlap and supports the appropriate coupling characteristics of the shoulder-couple structure.

To show the effectiveness of the shoulder-couple structure, shoulder-couple resonant-tunneling filters are tested. In Fig. 4(a), top and bottom waveguides are used as an input port and an output port, respectively. The characteristics of the filter are analyzed by the coupled-mode theory [15] where the transmittance (T) of the filter can be written as $(Q_T/Q_H)^2$. For the shoulder-couple structure of separation 9, the quality factor and the transmittance are 1.9×10^5 and 0.88, respectively. In case of the separation 11, $Q=9.7\times10^5$ and T=0.48. These performances compare favorably with those ($Q\sim10^4$) of previous works [6-8].

#5765 - $15.00 US Received 17 November 2004; revised 13 December 2004; accepted 16 December 2004

6. Butt-couple structure

The butt-couple structure and the field distribution are shown in Fig. 5(a). Two terminated Γ-K waveguides approach the waist of the hexapole mode from left and right. The separation is represented as the number of air-hole rows between the center of the cavity and the end of the PhC waveguide. For example, the separation is 7 in Fig. 5(a). The hexapole mode has an odd symmetry with respect to the Γ-K waveguide axis. However, the parity of the PhC waveguide mode is even as shown in Fig. 3(d). Because of the symmetry mismatch, no coupling between the modes is expected. In other words, the Q_H is infinite for all separations, indicating forbidden coupling between the hexapole mode and the even waveguide-mode.

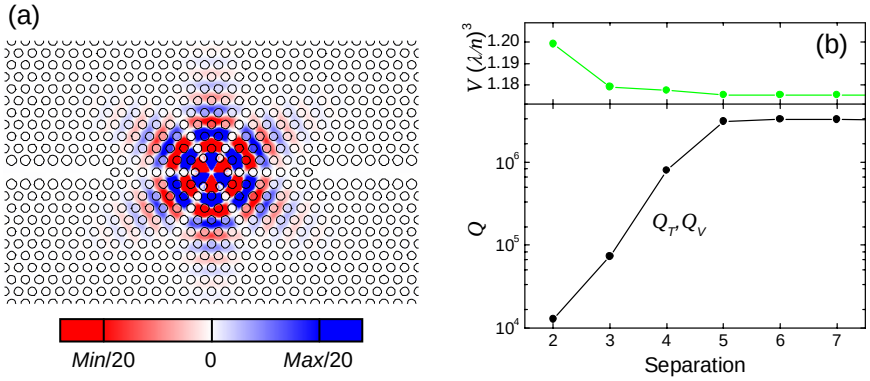

Fig. 5. (a) Butt-couple structure of separation=7 with H_Z distribution. (b) Modal volume (V) and quality factors (Qs) of hexapole mode. Green line represents modal volume. Black line represents the identical total and vertical Qs.

However, in spite of the forbidden coupling, the modal characteristics are still be affected by the dielectric perturbation stemming from the presence of the nearby waveguides. For example, when the separation is 2~4, the Q_T is smaller than that of the isolated hexapole mode. When the separation is ≥5, the hexapole mode remains practically unchanged. In fact, the PhC waveguide mode hardly overlaps with the hexapole mode because the waveguide is aligned along the line of the minimum intensity as shown in Fig. 5(a). For comparison, in the shoulder-couple structure, the much larger separation of ≥15 is needed to achieve the characteristics (Q_T and V) almost identical to those of the isolated cavity mode. In certain applications, it could be advantageous if one is able to place PhC waveguides in closer proximity without perturbing the resonant mode in question.

7. Side-couple structure

The field distribution of a side-couple structure is shown in Fig. 6(a). The modal volume and quality factors are computed as a function of separation. The separation is the number of air-hole rows between the center of the cavity and the PhC waveguide. For example, the separation is 7 in Fig. 6(a). In most cases, the horizontal quality factor Q_H is hundreds times larger than the vertical quality factor Q_V. It means that major fraction of the hexapole-mode energy flows into air instead of the side PhC waveguide. With Fig. 4(b) and Fig. 6(b), one can compare the Q_Hs of the shoulder-couple and side-couple structures. We find that the shoulder-couple waveguide-mode exchanges photons more efficiently with the hexapole mode than the side-couple waveguide-mode. In the side-couple structure, the coupling between the hexapole mode and the even waveguide-mode is extremely weak. This is in strong contrast with previous works [6-8] that employed the side-couple type.

#5765 - $15.00 US Received 17 November 2004; revised 13 December 2004; accepted 16 December 2004

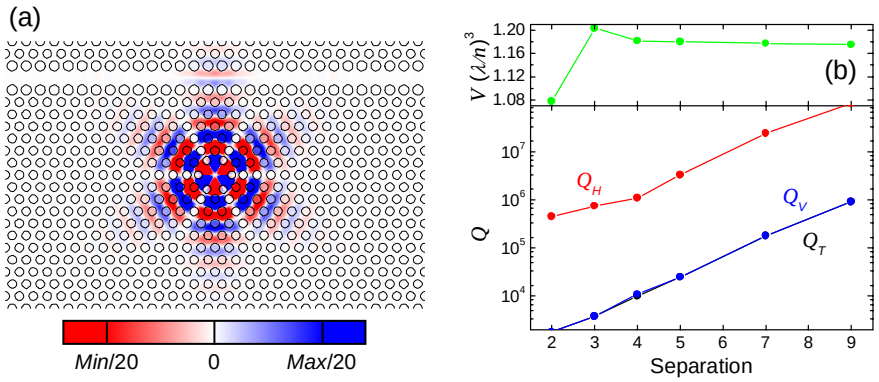

Fig. 6. (a) Side-coupled structure of separation=7 with H_Z distribution. (b) Modal volume (V) and quality factors (Qs) of hexapole mode. Green line represents modal volume. Black, red and blue lines represent total, horizontal and vertical Qs, respectively.

Characteristically the hexapole mode has six arms along Γ-M directions. Because the hexapole mode of this work is a donor-type mode, it is pulled down from the air-band edge of PhC slab. In the triangular-lattice PhC slab, the lowest-frequency mode of the air band is the characteristic M-point mode. Therefore, the characteristic signature of the mode profile originates from that of the air-band M-point mode. Among the six arms, the arm perpendicular to the waveguide axis overlaps most generously with the waveguide region of the side-couple structure as shown in Fig. 6(a) and determines the coupling characteristics. H_Z distributions of the dominant arm and the M-point mode are compared in Figs. 7(a) and 7(b). They have similar characteristics along the Γ-M direction. Note that the arm has the field profile with a quasi-odd symmetry inside the waveguide region. It becomes natural to relate this symmetry to the quasi-odd symmetric field distribution of the M-point mode. The PhC waveguide mode considered from the beginning of this work has an even symmetry. Therefore, the poor coupling in the side-couple structure is understandable by this symmetry argument.

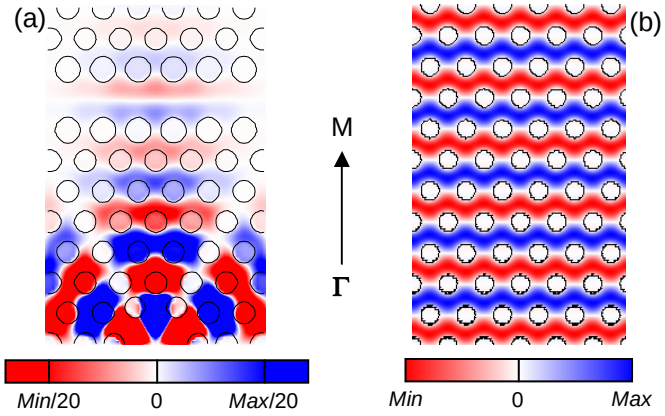

Fig. 7. (a) H_Z distribution of side-coupled structure showing the odd-like symmetry inside the waveguide. (b) Triangular-lattice photonic crystal and H_Z distribution of air-band M-point mode.

8. Conclusion

We have investigated the characteristics of the high-Q_V and small-V hexapole mode coupled with the even PhC-waveguide-mode. Three possible cavity-waveguide coupled structures are tested. The coupling efficiency shows strong dependence on the transverse overlap of the

#5765 - $15.00 US Received 17 November 2004; revised 13 December 2004; accepted 16 December 2004

cavity mode and the waveguide mode over the region of the waveguide. In the shoulder-couple structure, the hexapole mode smoothly couples to the even waveguide-mode maintaining the high Q_V and small V because the relative geometry of the hexapole-mode arm and the waveguide removes the possibility of symmetry mismatch. In the butt-couple structure, the hexapole mode does not couple with the even waveguide-mode because of the symmetry mismatch. In the side-couple structure, the coupling strength is much weaker as compared to the shoulder-couple structure because of the quasi-odd field distribution inside the waveguide region.

#5765 - $15.00 US Received 17 November 2004; revised 13 December 2004; accepted 16 December 2004